PAS3, a *Saccharomyces cerevisiae* Gene Encoding a Peroxisomal Integral Membrane Protein Essential for Peroxisome Biogenesis

Jörg Höhfeld, Marten Veenhuis,* and Wolf-H. Kunau

Institut für Physiologische Chemie, Abteilung für Zellbiochemie, Ruhr-Universität Bochum, D-4630 Bochum 1, Federal Republic of Germany; and *Laboratory for Electron Microscopy, University of Groningen, Biological Centre, 9751 NN Haren, The Netherlands

Abstract. *Saccharomyces cerevisiae* pas3-mutants are described which conform the pas-phenotype recently reported for the peroxisomal assembly mutants pasl-1 and pas2 (Erdmann, R., M. Veenhuis, D. Mertens, and W.-H Kunau. 1989. *Proc. Natl. Acad. Sci. USA.* 86:5419–5423). The isolation of pas3-mutants enabled us to clone the PAS3 gene by functional complementation. DNA sequence analysis revealed a 50.6-kD protein with at least one domain of sufficient length and hydrophobicity to span a lipid bilayer. To verify these predictions antibodies were raised against a truncated portion of the PAS3 coding region overexpressed in *E. coli*. Pas3p was identified as a 48 kD peroxisomal integral membrane protein. It is shown that a lack of this protein causes the peroxisome-deficient phenotype and the cytosolic mislocalization of peroxisomal matrix enzymes. Based on protease digestion experiments Pas3p is discussed to be anchored in the peroxisomal membrane by its amino-terminus while the bulk of the molecule is exposed to the cytosol. These findings are consistent with the possibility that Pas3p is one component of the peroxisomal import machinery.

In recent years the biogenesis of peroxisomes has attracted increasing attention. It is now widely accepted that peroxisomes arise by growth and division of preexisting organelles (Lazarow and Fujiki, 1985; Borst, 1986, 1989). Peroxisomal proteins are synthesized on free polyribosomes in the cytosol and posttranslationally imported into the organelle. In most cases, the translocation step occurs without covalent modification of the imported protein. The tripeptide SKL was identified as a peroxisomal targeting signal at the carboxyl terminus of different peroxisomal proteins by Gould et al. (1989). However, very little is still known about proteins that catalyze and control the biogenesis of peroxisomes.

In a recent report, we described the isolation of peroxisomal assembly mutants (pas-mutants) of *Saccharomyces cerevisiae* (Erdmann et al., 1989). These mutants were characterized by a lack of morphologically detectable peroxisomes and peroxisomal matrix enzymes were mislocalized to the cytosol. Phenotypically similar mutants were also isolated from CHO cells (Zoeller and Raetz, 1986; Tsukamoto et al., 1990) and from the methylotrophic yeast *Hansenula polymorpha* (Cregg et al., 1990). Special attention has been attracted to peroxisomal diseases in man, e.g., Zellweger syndrome (Schutgens et al., 1986). In cells of Zellweger patients, peroxisomal membrane ghosts were recently identified (Santos et al., 1988). The synthesis of peroxisomal matrix enzymes is unaffected in these cells, but the enzymes fail to be packaged within the membranes (Schram et al., 1986). It has been thus suggested that mutations in the peroxisomal import machinery cause these diseases (Santos et al., 1988).

The possibility to isolate pas-mutants of *S. cerevisiae* and the powerful genetic and molecular approaches available in this yeast make it an especially attractive organism in which to undertake a detailed molecular analysis of peroxisome biogenesis. This in turn may help to understand the severe peroxisomal defects in man. Here we report the isolation of three mutants of the pas3-complementation group. The affected gene has been cloned by functional complementation and characterized by sequence analysis. It is demonstrated that PAS3 encodes a 48-kD peroxisomal integral membrane protein essential for peroxisome biogenesis. A topological model of Pas3p within the membrane is discussed, which is in agreement with a possible function as a receptor protein.

Materials and Methods

Strains and Media

Bacterial and yeast strains used in this study are listed in Table I. Yeast complete and minimal media have been described earlier (Erdmann et al., 1989). YNO medium contained 0.1% oleic acid, 0.05% Tween 40, 0.1% yeast extract, and 0.67% yeast nitrogen base without amino acids; YPO medium contained 0.15% oleic acid, 0.05% Tween 40, 0.3% yeast extract, 0.3% bacto peptone, and 0.7% KH_2PO_4, adjusted to pH 6.0.

Isolation of pas3-mutants

Pas3-mutants were isolated after mutagenesis of X2180-1A (PM3-11, PM3-13) and UTL-7A cells (PM3-12) using ethyl methanesulfonate (Sherman et al., 1979). The screening protocol included replica plating on YNO-agar plates, fractionation of yeast cells, and EM as described by Erdmann et al. (1989). Mutants were characterized by standard yeast genetic techniques (Ausubel et al., 1989).

Table I. Yeast and Bacterial Strains

Strain	Genotype	Source or reference
Saccharomyces cerevisiae		
X2180-1A	*MATa, mal, gal2, SUC2, CUP1*	W. Duntze (Bochum)
XP300-26D	*MATα, ade2, trp5, his6, lys1, gal2*	W. Duntze (Bochum)
UTL-7A	*MATa, ura3-52, trp1, leu2-3*	W. Duntze (Bochum)
D273-10B	*MATα*	W. Duntze (Bochum)
XDC-10A	*MATα, ura3-52, trp1, leu2-3*	W. Duntze (Bochum)
PM3-11	*MATα, pas3, ura3-52, his6*	This study
PM3-12	*MATa, pas3, ura3-52, trp1, leu2-3*	This study
PM3-13	*MATα, pas3, ura3-52, trp1, leu2-3*	This study
GDP3-1–GDP3-9	*MATa, pas3::URA3, trp1, leu2-3*	This study
Escherichia coli		
TGI	*Δ(lac, pro) supE thi hsdD5 F' [traD36 pro⁺ lacI^q lacZΔM15]*	O. Pongs (Bochum)

Analytical Procedures

Acetyl-CoA acyltransferase (3-oxoacyl-CoA thiolase; EC 2.3.1.16), catalase (EC 1.11.1.6), 3-hydroxyacyl-CoA epimerase (EC 5.1.2.3), cytochrome c-oxidase (EC 1.9.3.1), and fumarate hydratase (fumarase; EC 4.2.1.2) were assayed by established procedures (Moreno de la Garza et al., 1985; Veenhuis et al., 1987).

EM

$KMnO_4$ fixation of intact yeast cells and catalase cytochemistry with 3,3'-DAB were performed as described by Erdmann et al. (1989). Immunocytochemistry on ultrathin sections of Lowicryl-embedded cells with anti 3-oxoacyl-CoA thiolase antibodies was performed as described by Douma et al. (1985).

Cloning and Characterization of PAS3

To isolate the PAS3 gene, the strain PM3-11 was transformed with a genomic DNA library of *Saccharomyces cerevisiae* contained in the *E. coli*-yeast shuttle vector YCp50 (Rose et al., 1987). Transformation was done by a modified lithium acetate method (Gietz and Sugino, 1988). Ura$^+$ transformants were screened on YNO-agar plates at 30°C for their ability to utilize oleic acid as sole carbon source. The complementing plasmid YCpP3/7.5 was recovered by a common isolation procedure (Ausubel et al., 1989). Subclones of YCpP3/7.5 were constructed by introducing defined restriction fragments and fragments obtained through partial digestion of the genomic insert with Sau3AI into the CEN4-URA3 vector pRS316 (Sikorski and Hieter, 1989). Complementation analysis involved transformation of the resulting plasmids into PM3-11, selection for Ura$^+$, and subsequent screening on YNO-agar plates.

Recombinant DNA techniques, including enzymatic modification of DNA, fragment purification, bacterial transformation, and plasmid isolation were performed essentially as described by either Maniatis et al. (1982) or Ausubel et al. (1989).

DNA Sequencing

To sequence the 2-kb overlapping region of plasmids pRSP3/2.4 and pRSP3/2.3, restriction fragments of this region were subcloned into vector pBLUESCRIPT (Stratagene Cloning Systems, La Jolla, CA). Single-stranded sequencing templates were prepared from transformed TGI bacterial cells infected with M13R408 as described (Stratagene Cloning Systems). Nucleotide sequence analysis was carried out using the dideoxy chain termination method (Sanger et al., 1977). The inferred Pas3p sequence was used to search EMBL Nucleotide Sequence Database rel. 25 for similarities with other known protein sequences using the GENPRO-program (Riverside Scientific Enterprise, Seattle, WA).

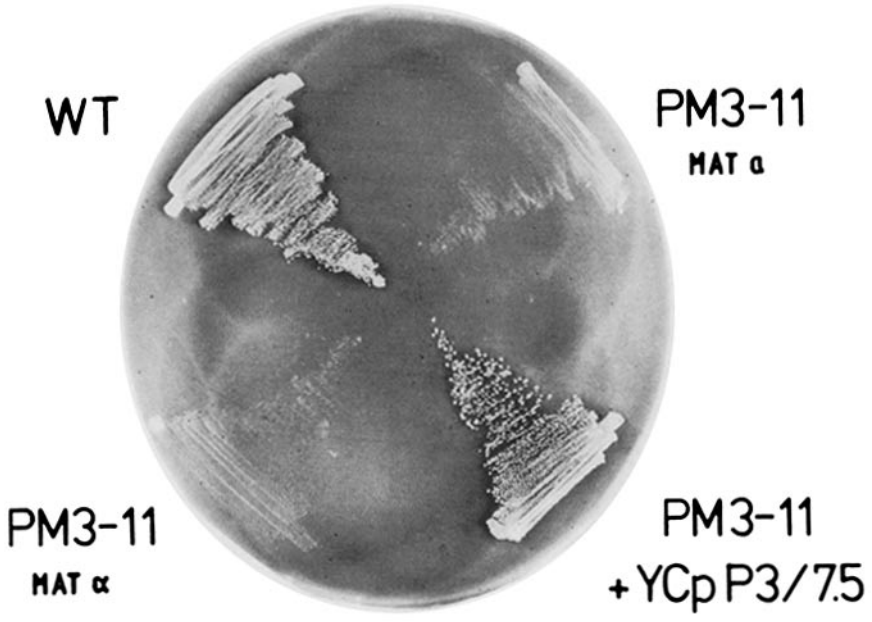

Figure 1. Screening for growth on oleic acid as sole carbon source. In contrast to the wild-type strain, two spores of PM3-11 are not able to grow on a YNO-agar plate after incubation at 30°C for 14 d. Transformation of PM3-11 with the plasmid YCpP3/7.5 results in a functional complementation of the oleic acid non-utilizing phenotype.

Integrative Disruption of PAS3

A 431-bp Sau3AI-EcoRI internal fragment of PAS3 was subcloned into a BamHI/EcoRI-digested shuttle vector YEp352 (Hill et al., 1986). The resultant plasmid was then digested with EcoRI/SalI and the released fragment was introduced into the integrative vector pRS306 (Sikorski and Hieter, 1989). The product of this manipulation, plasmid pRSP3-GD, contained the sequence of nucleotide 408–839 of PAS3. Plasmid pRSP3-GD was linearized with HindIII within the internal PAS3 sequence and subsequently used for transformation of UTL-7A. Ura^+ transformants were screened for onu^--phenotype and mated to XDC-10A. The diploids were sporulated and asci dissected into tetrads. The segregation of Ura^+ and onu^- was analyzed by replica plating. URA3:pas3 transformants were mated to PM3-11 and the resultant diploids checked for complementation.

Anti-Pas3p Antibodies

A 1.4-kb PstI-PstI fragment of pRSP3/2.3 was subcloned in frame into the *E. coli* expression vector pEXP1 (Raymond et al., 1990). The resultant plasmid contained a 1,293-bp fragment of PAS3 (lacking 30-bp at the 5′ end) behind the start codon of pEXP1. The construct produced a 455-residue polypeptide in response to the addition of isopropyl-β-D-thiogalactopyranoside to exponentially growing cultures (expression is under Ptac control in this vector system). Residues 1–24 are encoded by the start codon and multiple cloning site of pEXP1, whereas codons 25–455 encode amino acids 11–441 of Pas3p. After a 3-h induction of a transformed TG1 culture with 1 mM IPTG an additional protein band (M_r = 48 kD) was identified after SDS-PAGE (Laemmli, 1970) of bacterial lysates. The engineered polypeptide was essentially purified via the general procedure for insoluble protein aggregates (inclusion bodies) reported by Roberts et al. (1989). In contrast to the described procedure, the total cellular lysate was centrifuged for 10 min at 700 *g* and the pellet washed three times with 1% Triton X-100, 50 mM Tris, pH 7.5, and 20 mM EDTA, followed each time by centrifugation at 1,200 *g* for 10 min. The remaining pellet was resuspended in SDS-PAGE sample buffer and loaded on a 2-mm preparative SDS-polyacrylamide gel (10%). The purified polypeptide was transferred to a nitrocellulose membrane and the membrane slice dissolved in 500 μl dimethylsulfoxide. Antibodies were raised by primary subcutaneous injection of the solution (200 μg protein) into male New Zealand White rabbits. After 4 wk, 100-μg boost injections were administered subcutaneously every 3 wk until a satisfactory response was obtained.

Affinity Purification of anti-Pas3p Antibodies

The obtained antisera were affinity purified against a β-galactosidase-Pas3p fusion protein. The 1.4-kb PstI-PstI fragment of PAS3 was subcloned behind the lacZ gene of the expression vector pUR288 (Rüther and Müller-Hill, 1983). Induction of a transformed TG1 culture with IPTG led to the expression of a 165-kD fusion protein.

For affinity purification, crude extracts of the induced culture were loaded on a 10% SDS-polyacrylamide gel, transferred to a nitrocellulose membrane, and the 165-kD protein was cut out of the membrane sheet after staining with Ponceau S (Harlow and Lane, 1988). The membrane slice was incubated in 5% BSA for 30 min, washed several times with 50 mM Tris (pH 8.3), 150 mM NaCl containing 0.05% Tween 20 (TBS/Tween20) and incubated for 2 h in a 1:500 dilution of the crude antiserum. After intensive washing with TBS/Tween 20, the bound antibodies were eluted with 0.1 M Glycin, pH 2.5, 0.1% BSA and subsequently buffered with 0.25× vol. of 1 M Tris, pH 7.4, 0.1% BSA. The remaining membrane slice was washed with TBS/Tween 20 and again incubated in diluted antiserum. The affinity purified antibody was dialyzed against TBS/Tween 20 at 4°C and stored at −20°C.

Immunoblots

Western blot analysis was performed according to standard protocols (Harlow and Lane, 1988), using anti-rabbit IgG coupled alkaline phosphatase as second antibody (Sigma Chemical Co., St. Louis, MO). For detection of Pas3p, nitrocellulose filters were incubated overnight in the undiluted affinity-purified antibody at 23°C. Samples of yeast crude extracts were prepared for gel electrophoresis as described by Yaffe and Schatz (1984).

Fractionation of Yeast Lysates

Preparation and fractionation of yeast lysates by differential centrifugation was performed as already described (Erdmann et al., 1989). For further subfractionation by isopycnic sucrose density gradient centrifugation, wild type strain D273-10B was grown for 40 h on YPD medium, collected by centrifugation, and transferred to YPO medium (4 g wet weight per 500 ml medium). After inoculation for 18 h at 30°C, preparation and fractionation of the induced yeast cells were done as described by Erdmann et al. (1989). The resulting 25,000-*g* pellet fraction (35 mg protein) was resuspended in 6 ml 5 mM Mes buffer (pH 6.0) containing 0.5 mM EDTA, 0.6 M sorbitol, and 1 mM PMSF and loaded onto a continuous 32–54% sucrose density gradient (24 ml vol) with a cushion of 1 ml 60% sucrose dissolved in 5 mM Mes (pH 6.0), 1 mM EDTA, 1 mM KCl, 0.1% Ethanol. Centrifugation was performed for 1.5 h at 48,000 *g* in a Sorvall SS 90 vertical rotor at 4°C. After fractionation of the gradient, 100 μl of each fraction (total volume of 1 ml) was diluted in 900 μl 10% TCA and precipitated for 2 h on ice. The samples were centrifuged for 10 min in a microcentrifuge and the resulting pellet was resuspended in 50 μl Laemmli sample buffer with 2% β-mercaptoethanol (Laemmli, 1970). For Western blot analysis, 0.5–2 μl of each sample were loaded on a SDS-polyacrylamide gel.

Membrane Preparation

Membranes were prepared from isolated peroxisomes according to Fujiki et al. (1982) and Hashimoto et al. (1986), except that 1 mM PMSF was added to each solution. Centrifugation steps were performed at 200,000 *g* for 1 h.

Proteinase K Treatment

The 25,000-*g* pellet fraction (5 mg protein) of oleic acid induced wild-type cells was resuspended in 4 ml 1.2 M sorbitol, 5 mM Mes (pH 6.0) and divided into aliquots which were incubated at 30°C in the presence or absence of 25 mg/ml agarose-coupled proteinase K (Sigma Chemical Co.) and 0.1% Triton X-100. At different time points, aliquots of each sample were precipitated in 10% TCA and prepared for gel electrophoresis.

Table II. Distribution Pattern of Peroxisomal and Mitochondrial Marker Enzymes in the 25,000-g Supernatant and Pellet Fractions of Cell Lysates from Wild-type and pas3-Mutants Grown for 18 h on YNO Medium

Strain	Enzyme	Activity in 25,000 *g* Supernatant fraction (A1)	Activity in 25,000 *g* Pellet fraction (A2)	A1/A2
Wild-type	Thiolase	4.51	11.51	0.4
	Catalase	1.11 × 10^3	4.33 × 10^3	0.3
	Epimerase	3.17	20.14	0.2
	Fumarase	2.11	6.79	0.3
PM3-11	Thiolase	15.40	1.66	9.0
	Catalase	22.48 × 10^3	0.49 × 10^3	45.4
	Epimerase	5.32	1.24	3.2
	Fumarase	4.02	9.57	0.4
PM3-12	Thiolase	10.97	1.71	6.4
	Catalase	13.87 × 10^3	0.32 × 10^3	43.3
	Epimerase	12.97	4.10	3.2
	Fumarase	5.75	10.41	0.6
PM3-13	Thiolase	27.77	2.85	9.7
	Catalase	22.11 × 10^3	2.64 × 10^3	8.4
	Epimerase	12.73	3.60	3.5
	Fumarase	1.71	2.95	0.6
PM3-11 +YCpP3/7.5	Thiolase	5.22	14.11	0.4
	Catalase	1.81 × 10^3	3.06 × 10^3	0.6
	Epimerase	2.24	7.49	0.3
	Fumarase	2.22	7.52	0.3
GDP3-2	Thiolase	23.78	1.98	12.0
	Catalase	23.13 × 10^3	0.46 × 10^3	50.3
	Epimerase	15.26	3.86	4.0
	Fumarase	2.23	5.59	0.3

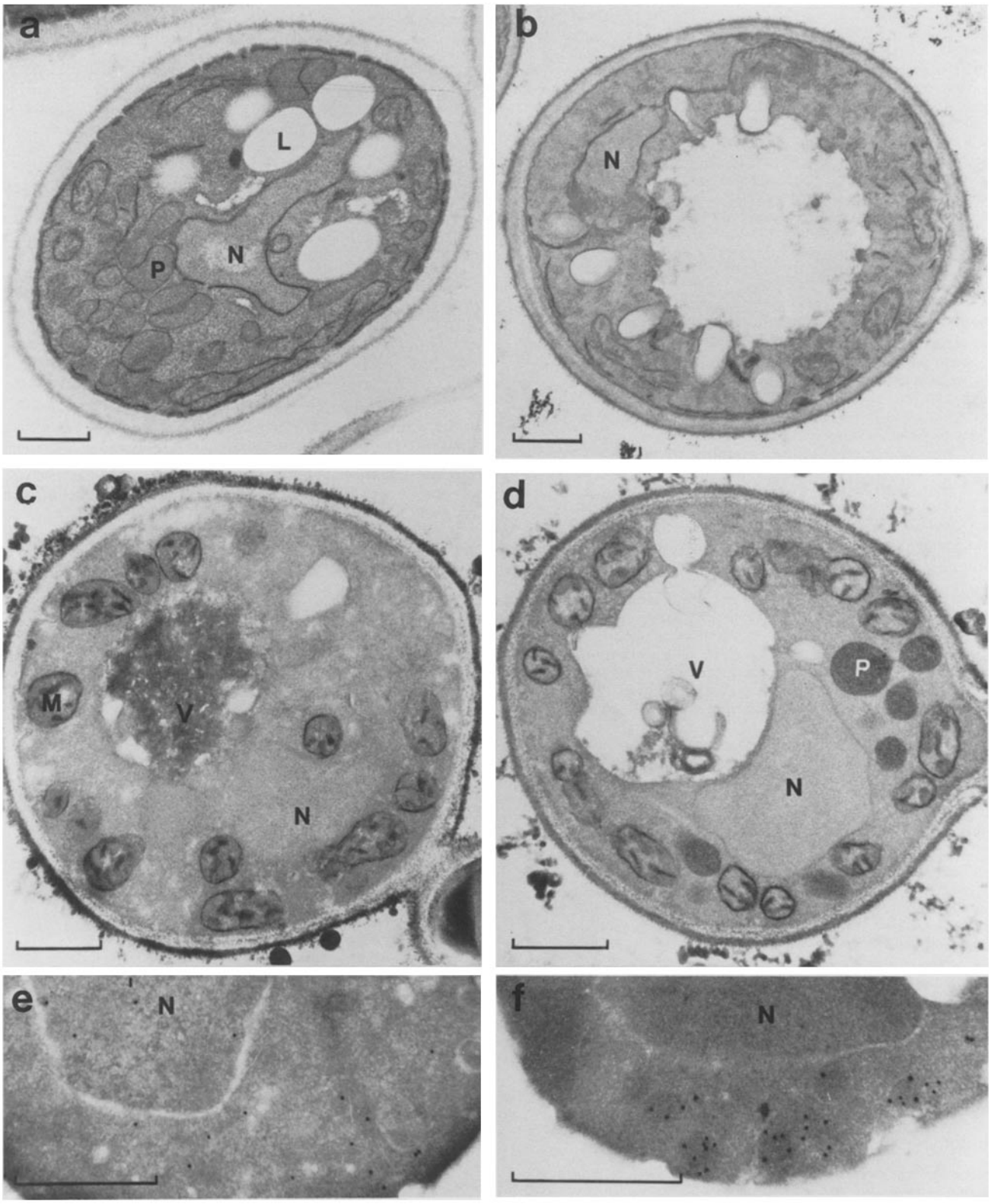

Figure 2. (*a* and *b*) Sections of $KMnO_4$-fixed oleic acid grown cells of wild-type *S. cerevisiae* (*a*) and the gene-disrupted strain GDP3-2 (*b*). In the case of the wild-type, growth on oleic acid resulted in a marked peroxisome proliferation (*a*). In contrast, peroxisomes were not detectable in sections of oleic acid–induced cells of the pas3-mutant GDP3-2 (*b*) grown under the same conditions as the wild-type strain. (*c–f*) The peroxisome-deficient morphology was also demonstrated by cytochemical staining of catalase activity. After incubation with DAB and H_2O_2, positively stained peroxisomal structures were absent in the mutant PM3-11 (*c*), but were readily detectable in PM3-11 cells transformed with the complementing plasmid YCpP3/7.5 (*d*). Immunocytochemical detection of thiolase revealed the particulate localization of this peroxisomal enzyme after functional complementation of PM3-11 (*f*), in contrast to nontransformed PM3-11 cells (*e*). *L*, lipid droplet; *M*, mitochondrion; *N*, nucleus; *P*, peroxisome; *V*, vacuole. Bar, 0.5 μm.

Results

Isolation and Characterization of pas3-mutants

We have previously described the isolation of four peroxisomal assembly mutants (pas-mutants) after mutagenesis of yeast wild-type cells with EMS (Erdmann et al., 1989). Genetic analysis revealed that these mutants fall into three complementation groups, pas1 to pas3 (Erdmann et al., 1989). In addition to the pas-defect the original pas3-mutant possessed a second mutation affecting the utilization of oleic acid as sole carbon source. As a first step to characterize the pas3-mutation a monogenic pas3-strain (PM3-11) was isolated by meiotic segregation. PM3-11 carries the pas3-defect as a single genetic lesion preventing growth on oleic acid as demonstrated by tetrad analysis. Backcrosses of PM3-11 to wild type cells yielded diploids that were able to utilize oleic acid indicating the recessive nature of the pas3-mutation. By means of the described screening procedure (Erdmann et al., 1989) two additional monogenic pas3-alleles (PM3-12, PM3-13) were isolated.

As described, peroxisomal assembly mutants of *S. cerevisiae* are not only characterized by their inability to utilize oleic acid as sole carbon source but, in addition, by the accumulation of peroxisomal matrix enzymes in the cytosol and by the absence of morphologically detectable peroxisomes (Erdmann et al., 1989). Therefore, the pas3-mutants were characterized with regard to these three properties before attempts to clone the PAS3 gene were initiated. The oleic acid nonutilizing phenotype (onu$^-$) demonstrated for all three pas3-mutants is shown for PM3-11 in Fig. 1. In contrast to a wild-type strain, the mutant is not able to grow on oleic acid minimal medium plates even after incubation for 14 d at 30°C.

It has been reported that not only pas-mutants but also strains defective in individual β-oxidation enzymes are unable to utilize oleic acid (Erdmann et al., 1989). Hence, further biochemical characterization was necessary to ensure that the onu$^-$-phenotype of PM3-11, PM3-12, and PM3-13 was due to a cytosolic mislocalization of peroxisomal enzymes. Subcellular fractionation studies were performed after induction on oleic acid medium. 3-hydroxyacyl-CoA epimerase and 3-oxoacyl-CoA thiolase, components of the peroxisomal β-oxidation system in yeast, and catalase were assayed as peroxisomal marker enzymes, while the mitochondrial enzyme fumarase served as a control for the intactness of the isolated organelles. Results are shown in Table II. For the wild-type strain, bulk activities of the different enzymes are present in the 25,000-*g* pellet, indicating their particulate nature. However, after differential centrifugation of lysates of PM3-11, PM3-12, and PM3-13, peroxisomal enzymes were predominantly detected in the 25,000-*g* supernatant, whereas the mitochondrial marker enzyme fumarase was still sedimentable (Table II). These data indicate that the biochemical phenotype of the pas3-mutants is the same as reported for pas1-1 and pas2: peroxisomal enzymes are still inducible; they are mislocalized to the cytosol, and they assemble in an active form (Erdmann et al., 1989).

The morphological phenotype of the pas3-mutants was investigated by EM. Growth of the wild-type strain on oleic acid as sole carbon source results in a marked peroxisomal proliferation (Fig. 2 *a*). In contrast, even after incubation with DAB and H_2O_2 for the detection of catalase activity, peroxisomes could not be detected in oleic acid induced cells of the pas3-mutant (Fig. 2 *c*). Staining of mitochondria is due to the activity of cytochrome c peroxidase. The cytosolic localization of peroxisomal matrix enzymes was also demonstrated by immunocytochemistry using polyclonal anti-thiolase antibodies (Fig. 2 *e*). It is to conclude that the pas3-mutation causes a lack of morphologically detectable peroxisomes.

Cloning of the PAS3 Gene by Functional Complementation

The recessive nature of the pas3-mutation opens the way to clone the PAS3 gene by functional complementation. PM3-11 was transformed with a genomic library of *S. cerevisiae* maintained in the *E. coli*-yeast shuttle vector YCp50 (Rose et al., 1987). Transformed cells were selected for uracil prototrophy and subsequently screened for growth on oleic acid medium. Among 30,000 transformants, one clone was recovered that had regained the ability to utilize oleic acid as carbon source (Fig. 1). The plasmid isolated from this clone (YCpP3/7.5) contained a 7.5-kb insert that was characterized by restriction analysis (Fig. 3). To verify that this plasmid carried the complementing gene, YCpP3/7.5 was transformed into PM3-11, PM3-12, and PM3-13. Ura$^+$ transformants of all mutant strains were again able to grow on oleic acid. Moreover, cell fractionation following oleic acid induction of the transformed mutant strains demonstrated the particulate localization of peroxisomal enzymes in these cells (Table II). The presence of peroxisomes was shown by catalase cytochemistry (Fig. 2 *d*) and the localization of 3-oxoacyl-CoA thiolase within these peroxisomes demonstrated by immunolabeling (Fig. 2 *f*). To localize the pas3-complementing region of YCpP3/7.5, subclones were constructed in pRS316 (Sikorski and Hieter, 1989) by using defined restriction fragments and fragments obtained through partial digestion with

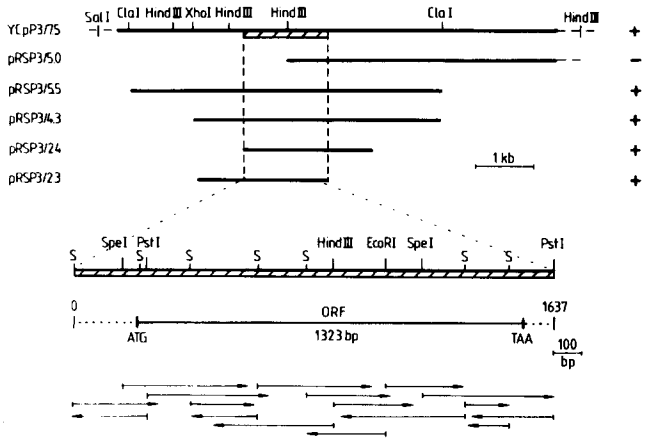

Figure 3. Complementation analysis and sequencing strategy of the *PAS3* region. The solid black line indicates the 7.5-kb genomic fragment of the plasmid YCpP3/7.5, which was found to complement the *pas3*-mutation. Subclones of this fragment are shown along with their complementing ability (−/+). The overlapping region of the different complementing subclones is marked with a hatched bar. A detailed restriction endonuclease map of this region and the identified large open reading frame is given in the lower panel. Arrows indicate the direction and extent of sequence determinations. *S*, Sau3AI site.

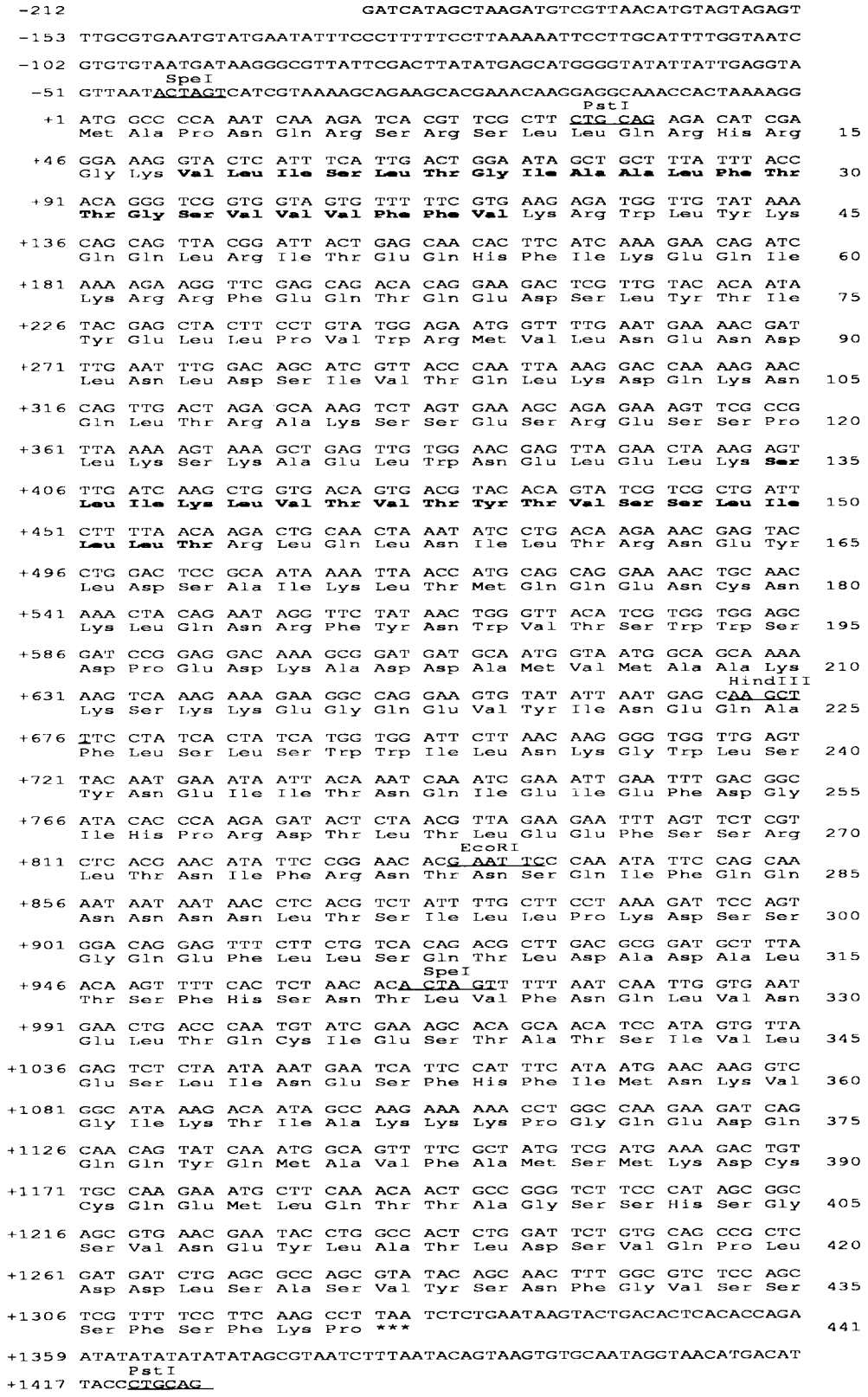

Figure 4. Nucleotide sequence of PAS3 and deduced primary sequence of the gene product. The two hydrophobic domains are shown shaded. The smallest complementing Sau3AI subclone starts at position −212 of the upstream region as was identified after partial Sau3AI digestion. For overexpression in *E. coli*, a portion of the gene from the PstI site at position +30 to the PstI site at +1420 was subcloned into the pEXP1 expression vector. These sequence data are available from EMBL/GenBank/DDBJ under accession number X58407.

Sau3AI. These subclones were tested for their ability to complement the onu⁻-phenotype of strain PM3-11. The results mapped the complementing gene to a region of ~2.0 kb (overlapping region between the complementing plasmids [Fig. 3]).

To establish the authenticity of the putative PAS3 gene and to exclude the possibility that a suppressor locus was cloned, a chromosomal integration experiment was performed. A 431-bp central Sau3AI-EcoRI fragment of the overlapping region was subcloned into the yeast integrating vector pRS306

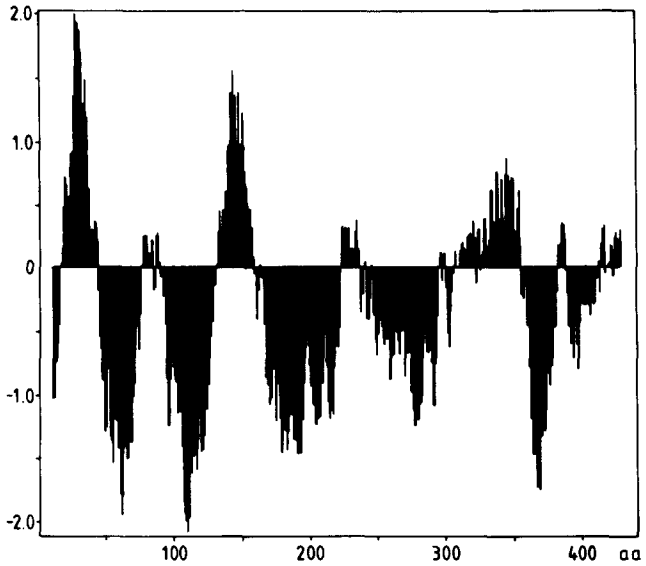

Figure 5. Hydropathy analysis of Pas3p. A hydropathy profile of the predicted amino acid sequence of Pas3p was calculated according to Kyte and Doolittle (1982) with a window size of 19 amino acids. Two hydrophobic regions were identified. The amino-terminal sequence (amino acid 18–39), especially, has been supposed to be a transmembrane span due to a length of 22 amino acids and a hydrophobicity score of about 2.0.

(Sikorski and Hieter, 1989). The resulting plasmid was linearized within the genomic fragment to direct integration to the homologous chromosomal locus. Subsequent transformation of haploid wild type cells yielded Ura$^+$ transformants (GDP3-1–GDP3-9) showing pas-phenotype (Table II, Fig. 2 *b*). GDP3-2 was mated to a wild type strain, resulting diploids were sporulated, and the meiotic segregation was examined by tetrad analysis. An absolute cosegregation of pas$^-$ and Ura$^+$ was observed. Moreover, a backcross of the disrupted haploid GDP3-2 to the original mutant PM3-11 led to diploids which were also not able to utilize oleic acid as carbon source. These results indicated an integration at the PAS3 locus of GDP3-2. Hence, the authentic PAS3 gene has been cloned.

Sequence Analysis of PAS3

The overlapping region between the genomic fragments of pRSP3/2.3 and 2.4 was sequenced using the dideoxynucleotide chain-termination method (Sanger et al., 1977). The sequenced stretch of 1,637 bp contains an open reading frame of 1,323 bp (Fig. 3), corresponding to a putative protein of 441 amino acids with a calculated molecular mass of 50.6 kD. Several features indicate that the first ATG codon of this open reading frame is indeed the translational start site. A putative TATA element was noted at position −74 relative to this ATG. In addition, the sequence CAAG, which often defines the start site of transcription (Dobson et al., 1982), was identified at position −23, and the flanking sequences fit well with the eukaryotic consensus sequence of translation start (Kozak, 1984) displaying an A at position −3 and a G at +4. An A-T rich region was found downstream of the TAA stop codon of the open reading frame. Such sequences have been proposed to be involved in the 3′-end formation of yeast mRNA by Zaret and Sherman (1982). A yeast consensus sequence for pre-mRNA splicing (Green, 1986) could not be identified. A transcript corresponding to the open reading frame was shown by a Northern blot using a specific fragment of PAS3 as a radiolabeled DNA-probe. Hybridization to poly (A)$^+$ mRNA isolated from oleic acid induced wild type cells led to the identification of a 1.5-kb mRNA species. In contrast, no signal could be detected when poly (A)$^+$ mRNA from glucose grown cells was used (data not shown). These results indicated that the open reading frame indeed encodes a polypeptide which is expressed in response to oleic acid induction.

Searching of EMBL Nucleotide Sequence Database rel. 25 revealed no significant sequence similarity to any other known protein sequence. Hydropathy analysis according to Kyte and Doolittle (1982) with a window size of 19 amino acids led to the identification of two hydrophobic regions within Pas3p (Fig. 5). Especially the amino terminal sequence (amino acids 18–39) fulfills the requirements for a membrane-spanning domain: a sequence of at least 19 amino acids with a hydrophobicity score higher than 1.6 (Kyte and Doolittle, 1982). The second stretch from amino acid 135 to 153 is characterized by a hydrophobicity score of 1.59. The nonpolar amino acids of this segment are disrupted by a lysine residue at position 138. Thus, it seems unlikely that this sequence acts as a second transmembrane span. Based on the

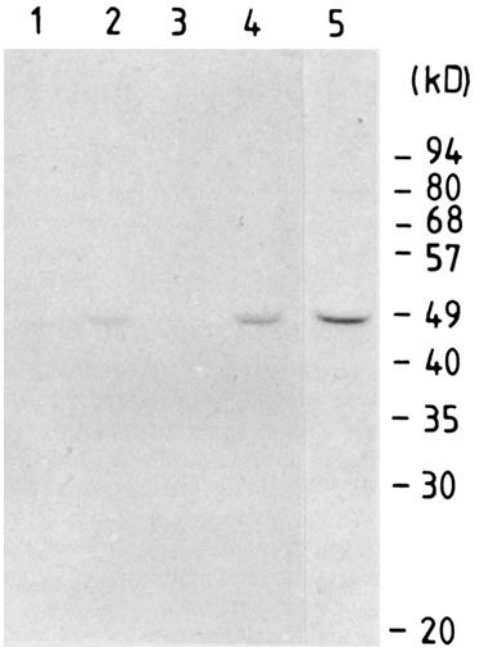

Figure 6. Identification of Pas3p. The Pas3p was identified in crude extracts of oleic acid induced wild-type cells by Western blot analysis using affinity-purified anti-Pas3p antibodies (lane *2*). In contrast, only a very weak signal was obtained in the crude extract of glucose grown cells (lane *1*). Oleic acid induction of a wild-type carrying additional copies of PAS3 on a multiple copy plasmid revealed an enhanced signal (lane *5*). After differential centrifugation of induced wild-type lysates, the Pas3p was exclusively found in the 25,000-*g* pellet fraction (lane *4*). (Lane *3* corresponds to the 25,000-*g* supernatant.)

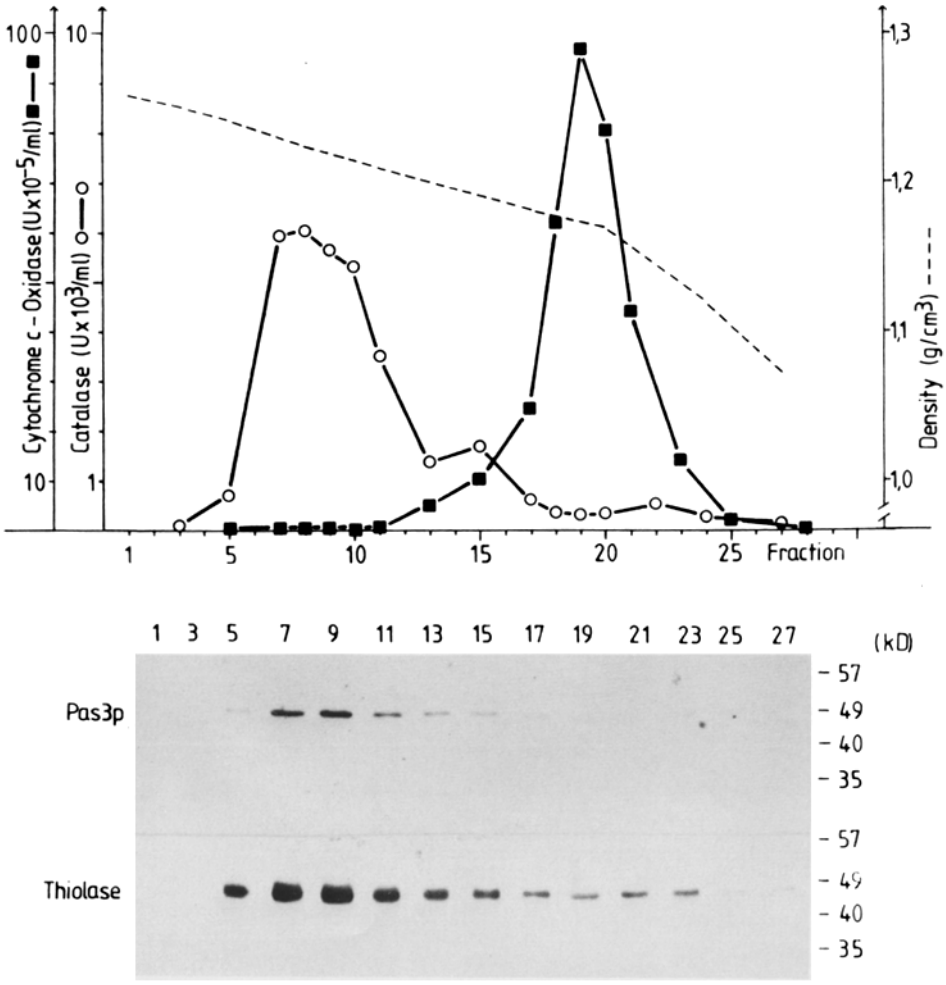

Figure 7. Immunological detection of Pas3p in peroxisomes. Peroxisomes were separated from mitochondria on a continuous 32–54% sucrose gradient as was indicated by the profiles of catalase and cytochrome c-oxidase activity. Peroxisomes were obtained at a density of 1.23 g/cm³, mitochondria at 1.18 g/cm³. The Pas3p was clearly detected in the peroxisomal peak fractions (7–10) by Western blot analysis. For the blot, 0.4% of the volume of each fraction was loaded onto a SDS-polyacrylamide gel. As a further control, fractions were also checked for the presence of the peroxisomal matrix enzyme 3-oxoacyl-CoA thiolase (each lane corresponds to 0.1% fraction volume).

hydrophobicity analysis, we predict that Pas3p is a membrane protein anchored by at least one membrane-spanning domain.

Identification and Intracellular Localization of Pas3p

The PAS3 nucleotide sequence data predicted a molecular mass of 50.6 kD for the gene product. Furthermore, the data indicated that Pas3p might be a membrane-bound protein. Analysis of these predictions was facilitated by the preparation of a specific antiserum. The product of a truncated PAS3 gene expressed in *E. coli* was purified as an insoluble inclusion body and used to generate anti-Pas3p antibodies in rabbits. For the experiments described in this study, the antiserum was used after affinity purification against a β-galactosidase-Pas3p fusion protein. As demonstrated in Fig. 6, the antibodies specifically react with a 48-kD polypeptide which is present in a very low amount when cells are grown on glucose (Fig. 6, lane *1*) and inducible by oleic acid (Fig. 6, lane *2*). Moreover, in a crude extract of oleic acid grown cells containing PAS3 on a multicopy plasmid an enhanced signal was obtained (Fig. 6, lane *5*), indicating that the 48-kD protein is the predicted PAS3 gene product. After a 25,000-*g* centrifugation of a yeast lysate obtained from spheroplasts, the protein was exclusively detected in the pellet fraction, suggesting a particulate localization of Pas3p (Fig. 6, lanes *3* and *4*). In contrast to this strong reaction in the 25,000-*g* pellet of the wild type lysate, it was not possible to immunologically detect the 48-kD protein in subcellular fractions of any of the three pas3-mutants PM3-11 to PM3-13 (data not shown). In addition, this was also the case for the gene-disrupted strain GDP3-2, providing further experimental evidence for the authenticity of the 48-kD protein as the PAS3 gene product. It can be concluded that the cause for the pas3-phenotype is a lack of this protein in the mutant strains. Although the experimental results strongly suggest that the immunoreactive 48-kD protein is indeed Pas3p, there is a difference of ~2.5 kD between the predicted and the apparent molecular mass. This might be explained by the frequently observed fact that hydrophobic proteins run with increased mobility in SDS-polyacrylamide gels (Büchel et al., 1980; Kamijo et al., 1990).

To further investigate the subcellular localization of Pas3p, a sucrose density gradient centrifugation was performed. The 25,000-*g* pellet fraction was subfractionated by isopycnic centrifugation in a 32–54% continuous sucrose density gradient. Fractions were analyzed for catalase activity as a peroxisomal marker enzyme, and cytochrome c-oxidase activity to detect mitochondria. Fig. 7 shows the distribution pattern of these enzymes. A clear separation of peroxisomes and mitochondria was achieved under these conditions. Peroxisomes were obtained at a density of 1.23 g/cm³,

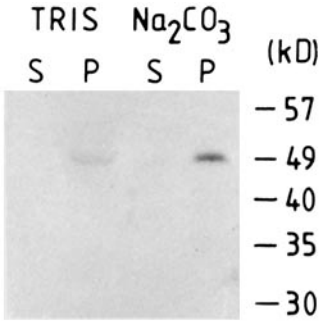

Figure 8. Immunological detection of Pas3p in the pellet fraction of carbonate-extracted peroxisomal membranes. Membranes were prepared from isolated peroxisomes by treatment with 10 mM Tris, pH 8.0. After 200,000 *g* centrifugation the resulting pellet fraction was extracted with sodium carbonate at pH 11.5 followed by a second centrifugation step (200,000 *g*, 1 h). The 48-kD Pas3p was identified in the pellet fractions as it is expected for an integral membrane protein. *S*, supernatant; *P*, pellet fraction.

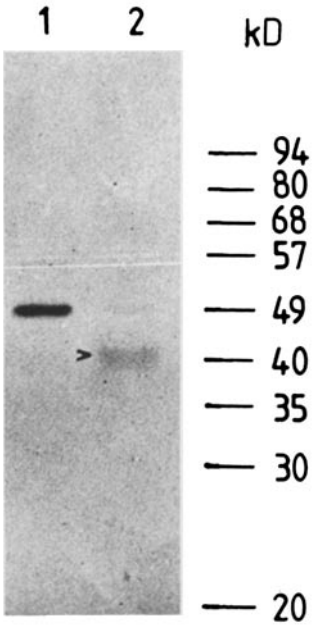

Figure 9. Degradation of Pas3p in peroxisomal gradient fractions stored at −20°C before membrane preparation. This degradation led to a 41-kD polypeptide (lane *2*, indicated by an *arrowhead*), which was specifically detected by affinity-purified anti-Pas3p antibodies. Lane *1* corresponds to the peroxisomal fraction of a sucrose gradient, lane *2* to the 200,000-*g* supernatant fraction after Na_2CO_3 extraction of peroxisomal membranes prepared from frozen peroxisomes.

whereas the mitochondrial fraction was found at a density of 1.18 g/cm³. The gradient fractions were further analyzed by Western blot analysis using polyclonal antibodies against the peroxisomal 3-oxoacyl-CoA thiolase and the affinity-purified anti-Pas3p antibodies. As shown in Fig. 7, the distribution pattern of both the 48-kD Pas3p and thiolase exactly follow the enzyme profile of the catalase activity. Based on these data, Pas3p can be characterized as a peroxisomal protein.

The hydropathy plot suggests that Pas3p is a membrane-bound protein. Especially the amino-terminal hydrophobic sequence seems to be long and hydrophobic enough to span a lipid bilayer. We further investigated this question by isolating peroxisomal membrane fractions by means of carbonate extraction (Fujiki et al., 1982). Peroxisomes isolated by sucrose density gradient centrifugation (see Fig. 7, fractions *7* and *8*) were lysed in 10 mM Tris, pH 8.0. A subsequent centrifugation at 200,000-*g* separated soluble from membrane-bound proteins. Incubation of the obtained pellet in Na_2CO_3 solution allowed to distinguish between peripheral and integral membrane proteins. The latter were found in the pellet fraction of a second 200,000-*g* centrifugation step. Immunoblot analysis (Fig. 8) demonstrates that the 48 kD Pas3p was a component of the 200,000-*g* pellet fraction after lysis of the organelles and was not extractable by carbonate. In this procedure it thus behaves like an integral membrane protein conforming the conclusion drawn from the hydropathy plot.

We have repeatedly observed a degradation of Pas3p when fractions from sucrose density gradients were stored at −20°C before membrane preparation. In these cases the 48-kD Pas3p was no longer detectable in peroxisomal membrane fractions. In contrast, the affinity-purified antibodies specifically reacted with a 41-kD polypeptide which behaved like a peripheral membrane protein; it was extractable from the Tris, pH 8.0 pellet fraction by carbonate treatment (data not shown). The specificity of the antibody reaction suggested that the 41-kD polypeptide is a degradation product of Pas3p (Fig. 9).

Protease Treatment of Pas3p

The topology of the 48-kD Pas3p in the peroxisomal membrane was examined by proteinase K treatment of a mitochondrial/peroxisomal pellet fraction (25,000-*g* pellet). Agarose-coupled proteinase K was used for this experiment and the organelles were osmotically stabilized in 1.2 M sorbitol during protease treatment. As a control that peroxisomal matrix enzymes were protected against the added protease by the membrane of the organelle, we investigated the protease sensitivity of 3-oxoacyl-CoA thiolase in the presence and absence of Triton X-100 by Western blot analysis. As shown in Fig. 10 a proteolytic digestion of thiolase was only observed when the organelles were lysed with Triton X-100 before the addition of proteinase K. In that case a polypeptide shortened by 3 kD was detected after a 10-min protease treatment and was further digested during incubation. Degradation products of smaller molecular mass were observed when larger amounts of protein were loaded onto the gel (data not shown). On the other hand, no cleavage of this peroxisomal matrix enzyme was observed in the absence of detergent, thus, indicating that the peroxisomal membrane remained intact under these experimental conditions.

In contrast, addition of proteinase K led to a complete degradation of Pas3p in the absence as well as in the presence of Triton X-100 (Fig. 10). In both cases, the Pas3-protein band disappeared after a 30-min incubation and a dominant cleavage product of 27 kD could be immunologically identified, which in turn was also rapidly degraded. Thus, the major part of Pas3p is apparently not protected from proteolytic attack by virtue of the intactness of the peroxisomal membrane.

Discussion

Very little is known about the functional features and structures of yeast peroxisomal membrane proteins. We report here the identification and molecular characterization of the peroxisomal integral membrane protein Pas3p which is essential for the biogenesis of peroxisomes in *Saccharomyces cerevisiae*. Cloning and sequencing of its gene, PAS3, became possible after the isolation of pas3-mutants.

All three reported pas3-mutants as well as the constructed null mutant revealed the same phenotype as the recently described strains pas1-1 and pas2 (Erdmann et al., 1989). This pas-phenotype is characterized by the lack of morphologically detectable peroxisomes, causing the inability of the

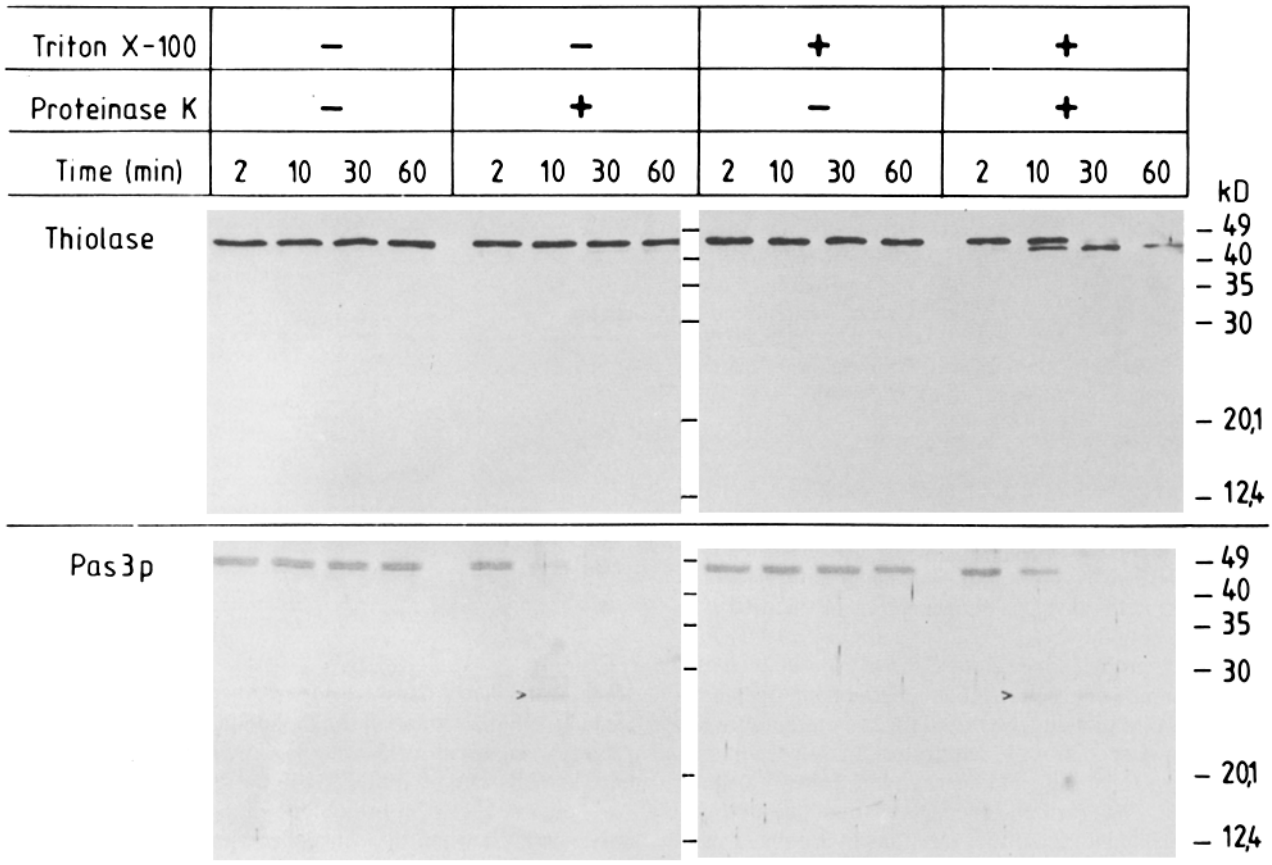

Figure 10. Western blot analysis using antibodies against 3-oxoacyl-CoA thiolase and Pas3p after proteinase K treatment of a crude organellar pellet fraction. Four samples of a 25,000-*g* pellet fraction of oleic acid–induced wild-type cells were incubated in the absence (−) or presence (+) of 25 mg/ml agarose-coupled proteinase K and 0.1% Triton X-100 at 30°C. After 2, 10, 30, and 60 min, aliquots of each sample were precipitated in 10% TCA and prepared for SDS-PAGE. In the case of the peroxisomal matrix enzyme thiolase, degradation during protease treatment was only observed when the organelles were lysed by the addition of Triton X-100. In contrast, Pas3p was accessible to the added proteinase K in the presence as well as in the absence of detergent. A 27-kD polypeptide was detected as the dominant cleavage product (indicated by *arrowheads*).

yeast cells to utilize oleic acid as sole carbon source. In addition, peroxisomal matrix enzymes, which are still inducible by oleic acid, are mislocalized to the cytosol. The same features have also been reported for peroxisome deficient mutants of CHO cells (Zoeller et al., 1989), and of *Hansenula polymorpha* (Cregg et al., 1990), as well as for fibroblasts of Zellweger patients (Schutgens et al., 1986; Schram et al., 1986). Interestingly, in Zellweger fibroblasts empty peroxisomal membrane structures ("ghosts") containing peroxisomal membrane proteins have been identified, indicating that defects of the peroxisomal protein import machinery cause these diseases in man (Santos et al., 1988).

Although such structures could not yet be unequivocally demonstrated in the different pas-mutants of *S. cerevisiae*, we would like to postulate that they do exist and are an inherent additional feature of the pas-phenotype. This conclusion is primarily based on the following two observations. Firstly, transformation of pas3-mutants with plasmids bearing the PAS3 gene resulted in strains with detectable peroxisomes (Fig. 2, *d* and *f*). Secondly, genetic crossing of haploid cells of pas3-mutants with strains of other pas complementation groups (e.g., pas1 or pas2) led to diploid cells containing peroxisomes. Accumulated evidence strongly suggests that peroxisomes do not form by a de novo assembly mechanism, but arise from pre-existing organelles by growth and division (Lazarow et al., 1985; Borst, 1986, 1989). In the light of this notion and the demonstration of ghosts in fibroblasts of Zellweger patients, our findings make it extremely unlikely that in yeast cells without residual peroxisomal remnants, recovery of an essential gene by itself can restore biogenesis of peroxisomes. The cloning of the PAS3 gene, encoding an integral peroxisomal membrane protein (see below) now provides the basis for strategies to search for peroxisomal ghosts in *S. cerevisiae* by means of molecular probes.

The sequence of the PAS3 gene predicts a 50.6-kD protein (Pas3p) that contains at least one stretch of amino acids 18–39 which is sufficiently long and hydrophobic to span a lipid bilayer. The predictions of the sequence analysis are strongly supported by the properties and the subcellular localization of the immunologically detected Pas3p. It is clearly identified as a peroxisomal protein of an apparent molecular mass of 48 kD and, judged by the carbonate-extraction method (Fig. 8), an integral component of the peroxisomal membrane. So far no integral peroxisomal membrane protein of *S. cerevisiae* and only three of other organisms, namely PMP70 of rat liver (Kamijo et al., 1990), PMP47 of *Candida boidinii* (McCammon et al., 1990*a*), and PAF-1 of CHO cells (Tsukamoto et al., 1991) have been

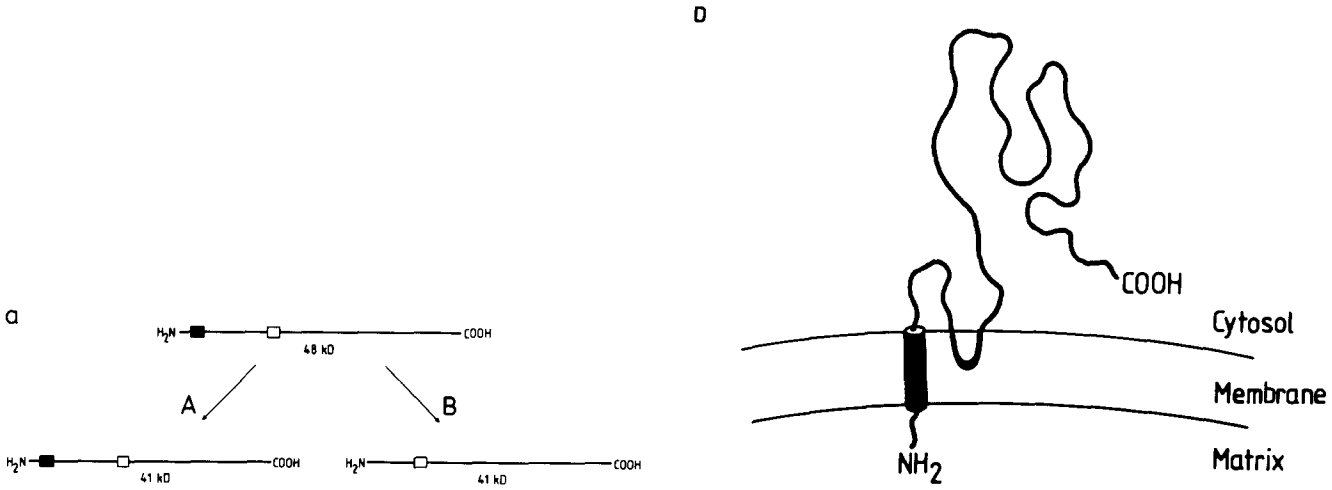

Figure 11. (*a*) Schematic presentation of alternative cleavages leading to the observed 41-kD degradation product of Pas3p (*48 kD*). (*A*) Putative cleavage at the hydrophilic carboxyl-terminus would result in a polypeptide containing both hydrophobic domains (shown as a *black and an open box*); (*B*) Putative degradation at the amino terminus would lead to a polypeptide missing the first hydrophobic stretch (*black box*) which is discussed as the membrane anchor of Pas3p. (*b*) Hypothetical model of the topology of Pas3p within the peroxisomal membrane.

characterized by cloning and sequencing of the corresponding genes. Comparison of their deduced amino acid sequences with that of Pas3p revealed no significant sequence similarity. While PMP70 and PMP47 were characterized as major integral peroxisomal membrane proteins in the respective organisms, a 48-kD protein was not among the predominant polypeptides of the peroxisomal membrane of *S. cerevisiae* (McCammon et al., 1990*b*).

With respect to the topology of Pas3p within the peroxisomal membrane, it was an interesting observation that a 41-kD degradation product of this protein (Fig. 9) behaved like a peripheral membrane protein. It is obvious from sequence analysis that a cleavage in the hydrophilic carboxyl-terminal half of Pas3p can not explain this finding (Fig. 11 *a, A*). However, the shift from an integral to a peripheral membrane protein and the size of the observed polypeptide could result from a cleavage between the two hydrophobic stretches of amino acids 18–39 and 135–153 (Fig. 11 *a, B*). The putative cleavage product would lack the first amino-terminal hydrophobic sequence which, as discussed above, possesses the properties of a membrane-spanning domain. This reasoning implies that the second hydrophobic stretch (amino acids 135–153) alone is not sufficient to anchor Pas3p in the lipid bilayer, but to peripherally associate it to the peroxisomal membrane. Further insight into the topology of Pas3p was obtained by protease treatment of a crude peroxisomal/mitochondrial pellet fraction. The easy accessibility of Pas3p to proteolytic attack even when membranes are not permeabilized by detergent (Fig. 10) suggests that the major portion of Pas3p protrudes into the cytosol. The size (27 kD) of the observed predominant degradation product corresponds well with the hydrophilic part of the Pas3-protein. Based on the presented data we have speculated about the topology of Pas3p (Fig. 11 *b*). It is presumably anchored in the lipid bilayer by the transmembrane domain at its amino terminus with its membrane association being supported by the second hydrophobic stretch, while the bulk of the molecule emerges from the cytosolic face of the peroxisomal membrane into the cytosol.

A search of databases failed to reveal significant sequence similarities of the deduced primary sequence of Pas3p to other known protein sequences, thus providing no insight into a possible function of this integral membrane protein. However, the discussed topology of Pas3p and its essential role for the biogenesis of peroxisomes are properties one would expect of a putative receptor on the peroxisomal membrane.

Fibroblast of Zellweger patients have been reported to contain peroxisomal membrane proteins in ghost-like structures (Santos et al., 1988), whereas soluble peroxisomal proteins were found in the cytosol of these cells (Schram et al., 1986). This seems to suggest that membrane-bound and soluble proteins are delivered to peroxisomes by separate mechanisms. It has recently been demonstrated that the tripeptide SKL and certain conservative modifications of this motif at the extreme carboxyl terminus of peroxisomal proteins function as a peroxisomal targeting signal in mammals, plants, and yeast (Gould et al., 1990). However, an SKL-like motif is absent at the carboxyl terminus of the deduced primary sequence of Pas3p as well as of PMP70 (Kamijo et al., 1990), PMP47 (McCammon et al., 1990*a*), and PAF-1 (Tsukamoto et al., 1991), the other known peroxisomal integral membrane proteins. Moreover, with respect to the discussed topology of Pas3p, with a membrane anchoring stretch at the extreme NH_2-terminus and the carboxyl-terminal half protruding into the cytosol, it is conceivable that the protein is directed to the peroxisomal membrane by an amino-terminal targeting signal.

Interestingly, the amino terminus of Pas3p shows a surprising structural similarity to the noncleavable NH_2 terminus of the 70-kD mitochondrial outer membrane protein of *S. cerevisiae* (Hase et al., 1984). In both cases there is only a short sequence preceding the hydrophobic transmembrane span, and this membrane spanning domain is surrounded by a number of basic residues. It was shown for the mitochondrial protein that the first 12 amino acids are sufficient for targeting to mitochondria, whereas the subsequent uncharged region up to residue 29 contains a "stop-transfer"

and "anchoring" function (Nakai et al., 1989). Based on these observations Pas3p should be a useful model protein for studies of integral membrane protein sorting to yeast peroxisomes.

We wish to thank Martina Marzioch and Ralf Erdmann for providing the noncharacterized pas3-mutants, and Klaas Sjollema and Jan Zagers for technical assistance concerning the electron micrographs. Plasmids pEXP1-3 were kindly provided by Tom Stevens, and plasmids pRS306/316 by Robert Sikorski and Philip Hieter. The YCp50 genomic bank was a generous gift of Carlos Gancedo. Special thanks are also extended to Franziska Wiebel and Daphne Mertens for helpful comments on the manuscript.

This work was supported by the Deutsche Forschungsgemeinschaft (Ku-329/3 and 329/4).

Received for publication 13 March 1991 and in revised form 20 May 1991.

References

Ausubel, F. J., R. Brent, R. E. Kingston, D. D. Moore, J. G. Seidman, J. A. Smith, and K. Struhl. 1989. Current Protocols in Molecular Biology. Greene Publishing Associates and Wiley-Interscience, New York.

Borst, P. 1986. How proteins get into microbodies. *Biochim. Biophys. Acta.* 866:179-203.

Borst, P. 1989. Peroxisome biogenesis. *Biochim. Biophys. Acta.* 1008:1-13.

Büchel, D. E., B. Gronenborn, and B. Müller-Hill. 1980. Sequence of the lactose permease gene. *Nature (Lond.).* 283:541-545.

Cregg, J. M., I. J. van der Klei, G. J. Sulter, M. Veenhuis, and W. Harder. 1990. Peroxisome-deficient mutants of *Hansenula polymorpha*. *Yeast.* 6:87-97.

Dobson, P., M. F. Tuite, N. A. Roberts, A. J. Kingsman, and S. M. Kingsman. 1982. Conservation of high efficiency promoter sequences in *Saccharomyces cerevisiae*. *Nucleic Acids Res.* 10:2625-2637.

Douma, A. C., M. Veenhuis, W. de Koning, and W. Harder. 1985. Dihydroxyacetone synthase is localized in the peroxisomal matrix of methanol-grown *Hansenula polymorpha*. *Arch. Microbiol.* 143:237-243.

Erdmann, R., M. Veenhuis, D. Mertens, and W.-H. Kunau. 1989. Isolation of peroxisome-deficient mutants of *Saccharomyces cerevisiae*. *Proc. Natl. Acad. Sci. USA.* 86:2432-2436.

Fujiki, Y., S. Fowler, H. Shio, A. L. Hubbard, and P. B. Lazarow. 1982. Polypeptide and phospholipid composition of the membrane of rat liver peroxisomes. *J. Cell Biol.* 93:103-110.

Gietz, R. D., and A. Sugino. 1988. New yeast-*E. coli* shuttle vectors constructed with in vitro mutagenized yeast genes lacking six-base pair restriction sites. *Gene.* 74:527-534.

Gould, S. J., G.-A. Keller, N. Hosken, J. Wilkinson, and S. Subramani. 1989. A conserved tripeptide sorts proteins to peroxisomes. *J. Cell Biol.* 108: 1657-1664.

Gould, S. J., G.-A. Keller, M. Schneider, S. H. Howell, L. J. Garrard, J. M. Goodman, B. Distel, H. Tabak, and S. Subramani. 1990. Peroxisomal protein import is conserved between yeast, plants, insects and mammals. *EMBO (Eur. Mol. Biol. Organ.) J.* 9:85-90.

Green, M. R. 1986. Pre-mRNA splicing. *Annu. Rev. Genet.* 20:671-708.

Harlow, W., and D. Lane. 1988. Antibodies - A Laboratory Manual. Cold Spring Harbor Laboratory, Cold Spring Harbor, New York. 726 pp.

Hase, T., U. Müller, H. Riezman, and G.Schatz. 1984. The 70 kd protein of the yeast mitochondrial outer membrane is targeted and anchored via its extreme amino terminus. *EMBO (Eur. Mol. Biol. Organ.) J.* 3:3157-3164.

Hashimoto, T., T. Kuwabara, N. Usuda, and T. Nagata. 1986. Purification of membrane polypeptides of rat liver peroxisomes. *J. Biochem.* 100:301-310.

Hill, J. E., A. M. Myers, T. J. Koerner, and A. Tzagoloff. 1986. Yeast *E. coli* shuttle vectors with multiple unique restriction sites. *Yeast.* 2:163-167.

Kamijo, K., S. Taketani, S. Yokota, T. Osumi, and T. Hashimoto. 1990. The 70 kDa peroxisomal membrane protein is a member of the Mdr (P-glycoprotein)-related ATP-binding protein superfamily. *J. Biol. Chem.* 265:4534-4540.

Kozak, M. 1984. Point mutations close to the AUG initiator codon affect the efficiency of translation of rat preproinsulin in vivo. *Nature (Lond.).* 308:241-246.

Kyte, J., and R. F. Doolittle. 1982. A simple method for displaying the hydropathic character of a protein. *J. Mol. Biol.* 157:105-132.

Laemmli, U. K. 1970. Cleavage of structural proteins during the assembly of the head of bacteriophage T4. *Nature (Lond.).* 227:680-685.

Lazarow, P. B., and Y. Fujiki. 1985. Biogenesis of peroxisomes. *Annu. Rev. Cell Biol.* 1:489-530.

Maniatis, T., E. F. Fritsch, and J. Sambrook. 1982. Molecular Cloning: A Laboratory Manual. Cold Spring Harbor Laboratory, Cold Spring Harbor, NY. 545 pp.

McCammon, M. T., C. A. Dowds, K. Orth, C. R. Moomaw, C. A. Slaughter, and J. M. Goodman. 1990*a*. Sorting of peroxisomal membrane protein PMP47 from *Candida boidinii* into peroxisomal membranes of *Saccharomyces cerevisiae*. *J. Biol. Chem.* 265:20098-20105.

McCammon, M. T., M. Veenhuis, S. B. Trapp, and J. M. Goodman. 1990*b*. Association of glyoxylate and beta-oxidation enzymes with peroxisomes of *Saccharomyces cerevisiae*. *J. Bacteriol.* 172:5816-5827.

Moreno de la Garza, M., U. Schultz-Borchard, J. W. Crabb, and W.-H. Kunau. 1985. Peroxisomal β-oxidation system of *Candida tropicalis*. *Eur. J. Biochem.* 148:285-291.

Nakai, M., T. Hase, and H. Matsubara. 1989. Precise determination of the mitochondrial import signal contained in a 70 kDa protein of yeast mitochondrial outer membrane. *J. Biochem.* 105:513-519.

Raymond, C. K., P. J. O'Hara. G. Eichinger, J. H. Rothman, and T. H. Stevens. 1990. Molecular analysis of the yeast VPS3 gene and the role of its product in vacuolar protein sorting and vacuolar segregation during the cell cycle. *J. Cell Biol.* 111:877-892.

Roberts, C. J., G. Pohlig, J. H. Rothman, and T. H. Stevens. 1989. Structure, biosynthesis, and localization of dipeptidyl aminopeptidase B, an integral membrane glycoprotein of the yeast vacuole. *J. Cell Biol.* 108:1363-1373.

Rose, M. D., P. Novick, J. H. Thomas, D. Botstein, and G. R. Fink. 1987. A *Saccharomyces cerevisiae* genomic plasmid bank based on a centromere-containing shuttle vector. *Gene.* 60:237-243.

Rüther, U., and B. Müller-Hill. 1983. Easy identification of cDNA clones. *EMBO (Eur. Mol. Biol. Organ.) J.* 2:1791-1794.

Sanger, F., S. Nicklen, and A. R. Coulson. 1977. DNA sequencing with chain-terminating inhibitors. *Proc. Natl. Acad. Sci. USA.* 74:5463-5467.

Santos, M. J., T. Imanaka, H. Shio, G. M. Small, and P. B. Lazarow. 1988. Peroxisomal membrane ghosts in Zellweger syndrome – aberrant organelle assembly. *Science (Wash. DC).* 239:1536-1538.

Schram, A. W., A. Strijland, T. Hashimoto, R. J. A. Wanders, R. B. H. Schutgens, H. van den Bosch, and J. M. Tager. 1986. Biosynthesis and maturation of peroxisomal β-oxidation enzymes in fibroblasts in relation to the Zellweger syndrome and infantile Refsum disease. *Proc. Natl. Acad. Sci. USA.* 83:6156-6158.

Schutgens, R. B. H., H. S. A. Heymans, R. J. A. Wanders, H. van den Bosch, and J. M. Tager. 1986. Peroxisomal disorders: a newly recognized group of genetic diseases. *Eur. J. Pediatr.* 144:430-440.

Sherman, F., G. R. Fink, and C. W. Lawrence. 1979. Methods in Yeast Genetics. Cold Spring Harbor Laboratory, Cold Spring Harbor, New York. 98 pp.

Sikorski, R. S., and P. Hieter. 1989. A system of shuttle vectors and yeast host strains designed for efficient manipulation of DNA in *Saccharomyces cerevisiae*. *Genetics.* 122:19-27.

Small, G. M., L. J. Szabo, and P. B. Lazarow. 1988. Acyl-CoA oxidase contains two targeting sequences each of which can mediate protein import into peroxisomes. *EMBO (Eur. Mol. Biol. Organ.) J.* 7:1167-1173.

Tsukamoto, T., S. Yokota, and Y. Fujiki. 1990. Isolation and characterization of Chinese hamster ovary cell mutants defective in assembly of peroxisomes. *J. Cell Biol.* 110:651-660.

Tsukamoto, T., S. Miura, and Y. Fujiki. 1991. Restoration by a 35K membrane protein of peroxisome assembly in a peroxisome-deficient mammalian cell mutant. *Nature (Lond.).* 350:77-81.

Veenhuis, M., M. Mateblowski, W.-H. Kunau, and W. Harder. 1987. Proliferation of microbodies in *Saccharomyces cerevisiae*. *Yeast.* 3:77-84.

Yaffe, M. P., and G. Schatz. 1984. Two nuclear mutations that block mitochondrial protein import in yeast. *Proc. Natl. Acad. Sci. USA.* 81:4819-4823.

Zaret, K. S., and F. Sherman. 1982. DNA sequence required for efficient transcription termination of yeast. *Cell.* 28:563-573.

Zoeller, R. A., and C. R. H. Raetz. 1986. Isolation of animal cell mutants deficient in plasmalogen biosynthesis and peroxisomal assembly. *Proc. Natl. Acad. Sci. USA.* 83:5170-5174.

Zoeller, R. A., L.-A. H. Allen, M. J. Santos, P. B. Lazarow, T. Hashimoto, A. M. Tartakoff, and C. R. H. Raetz. 1989. Chinese hamster ovary cell mutants defective in peroxisome biogenesis. *J. Biol. Chem.* 264:21872-21878.